

000 001 002 003 004 005 BT-MOE: A BUDGET-AWARE TUNING FRAMEWORK 006 FOR JOINT BIT-RANK ALLOCATION IN MOE MODELS 007 008 009

010 **Anonymous authors**
011 Paper under double-blind review
012
013
014
015
016
017
018
019
020
021
022
023
024
025
026

ABSTRACT

011 Quantization is a critical approach for efficiently deploying Mixture-of-Experts
012 (MoE) models with massive parameters. However, MoE models suffer from non-
013 negligible accuracy loss with extreme quantization, such as under 4 bits. To ad-
014 dress this, we introduce BT-MoE, a novel framework that achieves a unified and
015 globally optimal allocation of mixed-precision bit-widths and low-rank compen-
016 sator configurations. Our key insight is to formalize this co-design problem as
017 a Multiple-Choice Knapsack Problem (MCKP). To make this NP-hard problem
018 computationally feasible, we further propose an efficient proxy metric based on
019 layer-wise quantization loss for rapid configuration impact assessment, so that a
020 standard Integer Linear Programming (ILP) solver can solve the MCKP within
021 a practical time. Our comprehensive evaluation demonstrates that BT-MoE
022 consistently outperforms state-of-the-art quantization methods across various MoE
023 models and benchmarks. By systematically exploring the design space, BT-MoE
024 achieves superior accuracy-memory trade-offs, significantly improving the de-
025 ployability of large MoE models on resource-constrained hardware.
026

027 1 INTRODUCTION 028

029 The Mixture-of-Experts (MoE) architecture has emerged as the dominant paradigm for scaling Large
030 Language Models (LLMs), achieving state-of-the-art performance by replacing dense MLP blocks
031 with specialized expert networks and dynamic routing mechanisms (Jiang et al., 2024; Qwen et al.,
032 2025; Liu et al., 2024; Fedus et al., 2022). This design delivers enhanced model capacity without
033 sacrificing computational efficiency. However, these advantages come at the cost of critical deploy-
034 ment challenges. The memory footprint of MoE models is typically several times larger than dense
035 counterparts. For instance, Mixtral-8x7B requires approximately 88 GB of memory, which exceeds
036 the 24 GB capacity of consumer GPUs like RTX 4090, while DeepSeek-V3’s 671B parameters
037 surpass the memory capacity of eight H100 GPUs (Liu et al., 2024).

038 Deploying MoE models that exceed single-GPU memory requires either offloading to host or exter-
039 nal memory, which introduces additional communication overhead, or resorting to expensive multi-
040 GPU inference (Eliseev & Mazur, 2023; Rajbhandari et al., 2022). Among various compression
041 techniques, model quantization has emerged as the most promising approach for LLM deployment
042 (Frantar et al., 2022; Xiao et al., 2023; Badri & Shaji, 2023). Mixed-precision quantization further
043 enhances MoE model performance by assigning different bit-widths to model components based on
044 their quantization sensitivity (Huang et al., 2025b; Tang et al., 2024). This approach allocates lower
045 bit-widths to quantization-robust components while preserving higher precision for sensitive ones.

046 Despite these advances, a critical limitation emerges under aggressive compression scenarios. As
047 shown in Figure 1, while existing methods like GPTQ (Frantar et al., 2022) and HQQ (Badri & Shaji,
048 2023) maintain reasonable accuracy at 4-bit precision, they suffer severe performance degradation
049 when pushed to 3-bit quantization. For instance, Mixtral-8x7B experiences a perplexity increase
050 from 3.70 (FP16) to 4.73 (3-bit GPTQ), indicating a severe degradation in model performance.

051 To address this accuracy degradation, recent works have introduced low-rank compensators as post-
052 quantization correction mechanisms (Li et al., 2025a; Huang et al., 2025a). These methods capture
053 quantization residuals using low-rank matrix factorization, effectively recovering lost information.
However, existing approaches suffer from a fundamental design flaw: they treat bit-width selection

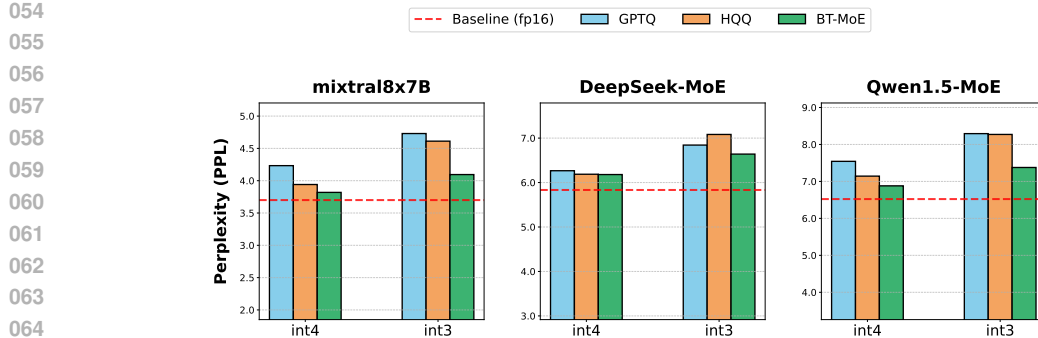


Figure 1: Comparison of existing quantization methods and BT-MoE on various bit-precision.

and compensator rank allocation as independent optimization problems, typically applying uniform configurations across all experts.

This uniform approach fundamentally misaligns with the heterogeneous nature of MoE architectures. Our empirical analysis reveals that different experts exhibit dramatically different sensitivities to quantization: some experts can tolerate aggressive 2-bit quantization with minimal accuracy loss, while others require higher precision even with compensator assistance. More critically, we discover a complex interdependency between bit-width and compensator rank: the optimal compensator rank for an expert is not fixed but depends heavily on its quantization bit-width, and vice versa. This interdependency creates a vast combinatorial optimization space that defies simple heuristic solutions. For a typical MoE model with 64 experts, each having 5 bit-width options and 5 rank choices, the total configuration space exceeds $25^{64} \approx 10^{90}$ possibilities, making exhaustive search computationally intractable. Existing greedy approaches, such as allocating the highest resources to the most frequently activated experts, fail to capture the nuanced trade-offs between different configuration combinations and often converge to local minima.

To address these challenges, we propose BT-MoE, a novel framework that introduces a Budget-Aware Tuning approach for the joint allocation of mixed-precision bit-widths and low-rank compensators. Our central idea is to cast the joint design as a Multiple-Choice Knapsack Problem (MCKP), where each expert selects exactly one configuration from a set of (bit-width, rank) candidates under a global resource budget. Although the resulting problem is NP-hard, we make it computationally tractable by employing an efficient layer-wise proxy for quantization-induced degradation. This proxy enables rapid evaluation of thousands of candidate configurations without exhaustive full-model retraining or validation, allowing the global selection to be solved by a standard Integer Linear Programming (ILP) solver within a practical time.

Our contributions are threefold. (1) We identify and formalize the complex coupling between weight bit-width and compensator rank in MoE quantization. (2) We propose an ILP-based global allocation method that jointly optimizes both dimensions, enabled by an efficient proxy metric that makes the global optimization computationally feasible. (3) We demonstrate consistent and significant improvements over existing methods across multiple MoE models and benchmarks, achieving superior accuracy-memory trade-offs that enable practical deployment of large MoE models on resource-constrained hardware.

2 RELATED WORKS

Post-Training Quantization (PTQ). PTQ has become the standard for LLM compression, avoiding the prohibitive cost of Quantization-Aware Training (QAT). In this line of work, state-of-the-art methods such as GPTQ (Frantar et al., 2022) and AWQ (Lin et al., 2024) have successfully compressed dense LLMs to 4-bit precision without significant accuracy loss. More recently, calibration-free methods like HQQ (Badri & Shaji, 2023) have also been explored, which capture outliers using a Super-Laplacian distribution with a closed-form solution. However, a uniform quantization scheme is often suboptimal for models with heterogeneous components like MoEs. To address this, Mixed-precision quantization allocates varied bit-widths to model components based on their differing sensitivities to quantization error (Wang et al., 2019; Dong et al., 2019). This principle is

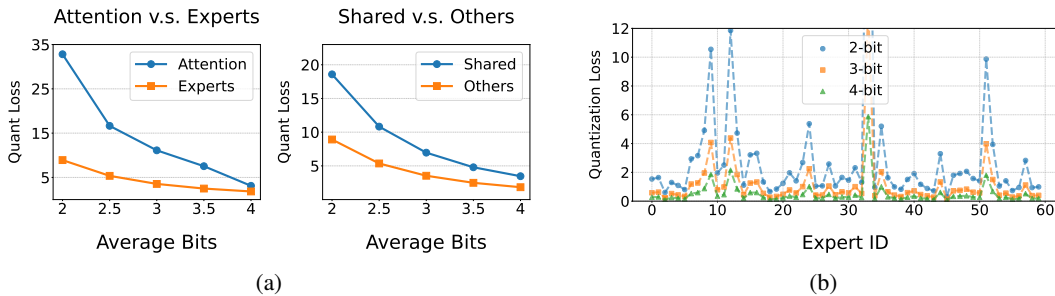
108 particularly effective for MoE models, whose experts naturally exhibit heterogeneous sensitivities
 109 (Huang et al., 2025b). Nevertheless, a key challenge persists: existing PTQ approaches, whether
 110 uniform or mixed-precision, still struggle to maintain accuracy when compressing MoE models to
 111 higher compression ratios, particularly in the sub-4-bit regime.

112 **Low-rank Compensation methods for LLM compression.** Low-Rank Factorization techniques
 113 are widely used to compensate for accuracy loss in LLM compression. ASVD (Yuan et al., 2023)
 114 proposes an activation-aware factorization method that uses a transformation matrix to absorb infor-
 115 mation about outliers from the activations into the weight matrices to compress the model. LoRC
 116 (Yao et al., 2024) applies low-rank factorization to the quantization error matrix and uses the low-
 117 rank matrices as a "compensator," making it an effective method for model accuracy recovery.
 118 SVDQuant (Li et al., 2025a) utilizes a high-precision, low-rank branch to absorb the most hard-
 119 to-quantize outliers in the weights and activations, thereby allowing the remaining, smoother resid-
 120 ual component to be easily quantized to 4-bit precision. MiLo (Huang et al., 2025a) designs a
 121 mixed-rank compensation scheme specifically for MoE models, adaptively assigning varying ranks
 122 to different experts. Different from those efforts, we explore a joint optimization of mixed-precision
 123 quantization and low-rank compensation for different components in MoE models, systematically
 124 exploring the optimal model compression configuration.

125 3 METHODOLOGY

126 3.1 CO-DESIGN CHALLENGE IN MOE QUANTIZATION

127 The core challenge in compressing MoE models lies in their heterogeneous nature. Different com-
 128 ponents exhibit varying sensitivities to quantization, creating a complex optimization space. Our
 129 analysis, along with recent studies, reveals a clear hierarchy of these sensitivities (Duanmu et al.,
 130 2025). As illustrated in Figure 2a, we observe that attention layers are more sensitive than expert
 131 FFNs, and shared experts are more sensitive than regular experts. Furthermore, within a single MoE
 132 layer, experts exhibit varying sensitivities to quantization (Figure 2b). This heterogeneity motivates
 133 the use of mixed-precision quantization.

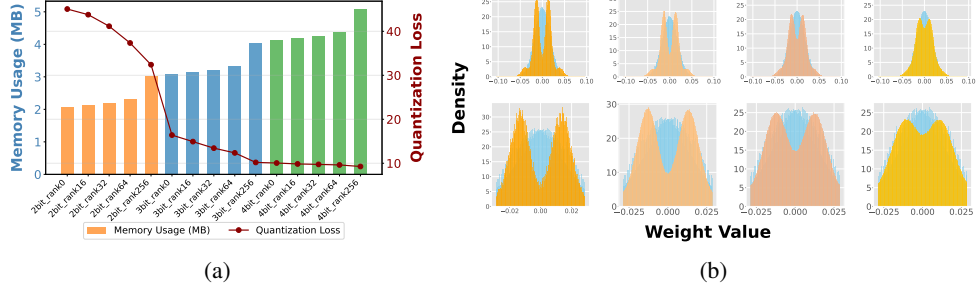


147 Figure 2: (a) Comparison of quantizing more bits for attention vs. experts and shared-experts v.s.
 148 others evaluated on the DeepSeek-MoE-16B-base model. (b) Quantization loss across experts in
 149 Qwen1.5-MoE's 1st layer under different bit width, group_size=128.

150 However, heuristic-based bit allocation (Li et al., 2025b) is insufficient, particularly under the ag-
 151 gressive compression required by strict memory budgets, which inevitably leads to significant quan-
 152 tization error. To counteract this residual error, low-rank compensators have been introduced as a
 153 powerful correction tool. It creates a second, coupled dimension for optimization: the rank of the
 154 compensator. However, the co-design of mixed-precision bit-widths and compensator ranks intro-
 155 duces three fundamental challenges:

156 **(1) Coupled Relationship: Nonlinear trade-offs between bit-width and rank.** The memory
 157 budgets for bit-width and rank compensation are interdependent. An expert quantized to a lower
 158 bit-width can have its accuracy recovered by a higher-rank compensator. We find that the benefit of
 159 increasing the compensator rank for an expert depends on its current quantization bit-width. For an
 160 expert quantized to 2-bit, a rank-32 compensator might provide a significant improvement; however,
 161 for an expert already at 4-bits, the same compensator may have little effect. As shown in Figure
 162 3(a), a 4-bit configuration with no compensator might yield a similar quantization loss to a 3-bit

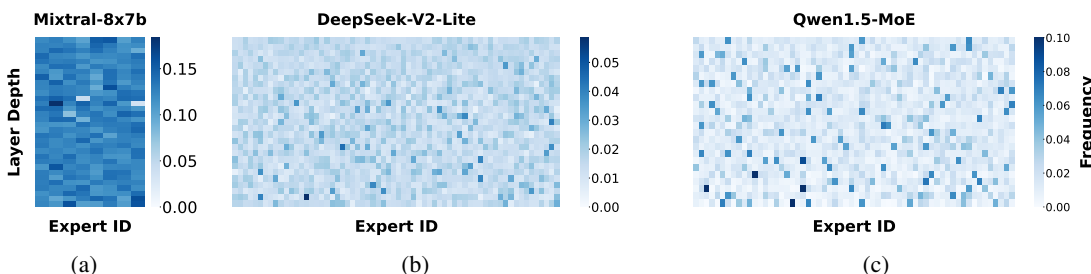
162 configuration with a rank-64 compensator, but the 4-bit configuration is more memory-intensive.
 163 This non-linear coupling between bit-width and rank indicates that optimizing one dimension in
 164 isolation will lead to a suboptimal outcome.



166
 167
 168
 169
 170
 171
 172
 173
 174
 175
 176
 177
 178
 179
 180
 Figure 3: (a) Quantization Loss vs. Memory Footprint for a single expert (Layer 10, Expert 24) in
 DeepSeek-V2-Lite under various compression configurations. (b) Weight distribution for a single
 expert (Layer 20, Expert 17) in Qwen1.5-MoE under 2-bit quantization, illustrating the accuracy
 recovery from different compensator ranks.

181 **(2) Heuristic Limitations: Greedy and frequency-based allocation fall short.** Due to the coupled
 182 relationship described above, employing simple greedy algorithms or heuristic strategies can easily
 183 lead to a local optimum. For example, allocating the highest-cost configuration (i.e., the highest
 184 bit-width and rank) to the most sensitive expert might seem reasonable, but this can excessively
 185 consume the budget. This would leave dozens of other experts with poor configurations, conse-
 186 quently harming the overall model performance.

187 Some existing work on mixed-precision MoE quantization uses a heuristic based on expert activation
 188 frequency; however, we find this approach also fails to achieve optimal results. This is particularly
 189 true for MoE models like Mixtral-8x7B. This is because the model has a small number of experts
 190 per layer, leading to little variance in their activation frequencies, as shown in Figure 4a. For models
 191 with a large number of fine-grained experts, such as DeepSeek-MoE and Qwen1.5-MoE, the expert
 192 activation frequencies exhibit significant variance, as shown in Figure 4b and 4c. Consequently, for
 193 these models, a frequency-based mixed-precision allocation can be a reasonably effective strategy.



194
 195
 196
 197
 198
 199
 200
 201
 202
 203
 204
 205
 Figure 4: Heatmap of expert activation frequency in Mixtral8x7B, DeepSeek-V2-Lite and Qwen1.5-
 MoE on the WikiText-2 task. The vertical axis from top to bottom represents the layer depth, and
 the horizontal axis represents expert indices.

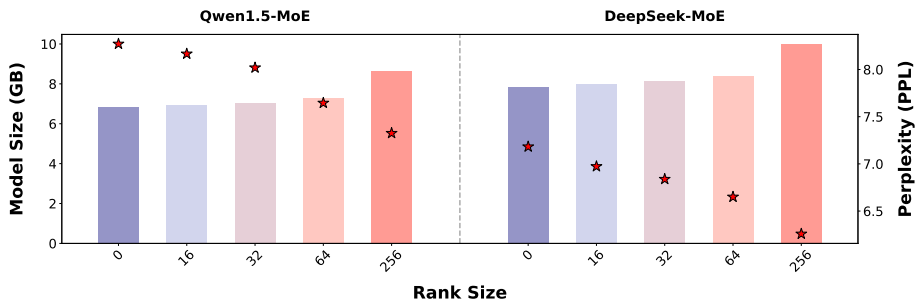
206 **(3) Combinatorial Explosion: Vast search space and costly evaluation.** A key difficulty in co-
 207 optimizing bit-width selection and compensator rank lies in the Combinatorial Explosion, which
 208 creates an extremely large design space. An MoE model contains a large number of experts, and
 209 each expert has multiple possible combinations of bit-widths and compensator ranks. For instance,
 210 models like Qwen1.5-MoE or DeepSeek-MoE have over 60 experts per layer. If we provide just
 211 a few bit-width options and several rank choices for each expert, every expert will have dozens of
 212 possible configurations. For the entire model, the total number of combined configurations is vast:

$$O\left((|\mathcal{B}| \times |\mathcal{R}|)^{|\mathcal{E}|}\right),$$

213 where \mathcal{B} is the number of bit-width options, \mathcal{R} is the number of rank options, and \mathcal{E} is the total
 214 number of experts in the model to be configured. making a brute-force search of all possibilities

216 computationally impossible. Therefore, this is a massive discrete combinatorial optimization prob-
 217 lem that requires a systematic method to efficiently explore this vast design space.
 218

219 This challenge is twofold. Beyond the sheer number of configurations, evaluating the quality of
 220 any single complete assignment by running a full model benchmark is also prohibitively expensive.
 221 To solve this, our framework introduces a two-part approach. First, to address the evaluation cost,
 222 we propose an efficient proxy metric based on layer-wise quantization loss. Through isolated per-
 223 turbation experiments, we rapidly collect the quant-loss for each expert under every potential (bit,
 224 rank) configuration. This allows us to model the global accuracy degradation as the weighted sum
 225 of these local losses. Second, with the cost and impact of each configuration now quantified, we
 226 tackle the search problem by formulating this task as an Integer Linear Programming (ILP) prob-
 227 lem. By minimizing the total weighted loss, the ILP solver can efficiently navigate the vast design
 228 space to find a provably optimal solution, bypassing the need for an exhaustive search. As our ex-
 229 periments demonstrate, this systematic approach yields configurations that are significantly superior
 to baseline methods.



240 Figure 5: Comparison of Model Size (GB) and Perplexity (PPL) for DeepSeek-V2-Lite and
 241 Qwen1.5-MoE at 3-bit precision with different compensator ranks and a group size of 128. The
 242 * symbols indicate corresponding perplexity values on WikiText2.
 243

244 3.2 ILP-BASED FRAMEWORK FOR UNIFIED GLOBAL ALLOCATION

246 Mixed-precision quantization and low-rank compensation are complementary techniques for com-
 247 pressing MoE models, yet integrating them within a single optimization framework remains nontriv-
 248 ial. To address the co-design challenges outlined in Section 3.1, we present BT-MoE, an ILP-driven
 249 framework that performs unified, global allocation of bit-widths and compensator ranks. BT-MoE
 250 formulates the joint selection as a constrained optimization problem over a discrete configura-
 251 tion space, enabling principled trade-offs between accuracy and resource usage and avoiding the sub-
 252 optimality of heuristic decisions.

253 3.2.1 OPTIMIZING UNIFIED (BIT, RANK) CONFIGURATIONS

255 The basic building block of our framework is the unified $(bit, rank)$ pair configuration assigned to
 256 each expert. To ensure each potential configuration is effective before our global search, we must
 257 optimally solve for its internal parameters. This involves finding the best possible balance between
 258 the precision offered by the bit-width and the error correction provided by the compensator rank.

259 To achieve this, we employ an iterative joint optimization process, inspired by MiLo (Huang et al.,
 260 2025a), which is superior to treating quantization and compensation as separate, sequential steps.
 261 For each candidate $(bit, rank)$ pair, we solve for the optimal quantization parameters (zero-point and
 262 scale) and compensator matrices (U, V) by minimizing the overall representation error:

$$263 \arg \min_{z,s,U,V} \mathcal{L}(W - Q_{z,s}^{-1}(Q_{z,s}(W)) - UV).$$

265 This optimization alternates between two key steps:

266 **(1) Quantization Optimization:** For the given bit-width, we treat the compensated weight matrix
 267 $W - UV$ as the target for quantization. We then apply an iterative solver based on HQQ to this
 268 target matrix to find the optimal quantizer parameters (z, s) .

269 **(2) Low-Rank Compensator Optimization:** For the given rank, we use Singular Value Decom-
 270 position (SVD) on the current quantization residual $W - W_q$ to find the optimal compensator matrices

(U, V). This process ensures that each configuration passed to our ILP solver is a locally-optimized implementation.

3.2.2 MODELING AS A MULTIPLE-CHOICE KNAPSACK PROBLEM

We model the task of assigning a (*bit, rank*) configuration to each expert as a Multiple-Choice Knapsack Problem (MCKP). This analogy provides a clear and powerful framework for our optimization:

- The Knapsack represents the total allowed memory budget for the compression overhead.
- Each Expert in the MoE model corresponds to a group of items.
- Each possible (*bit, rank*) Configuration for an expert is an item within that group (e.g., (3-bit, rank-32) is one item).
- The Value of an item is its contribution to accuracy, weighted by the **expert’s importance**.
- The Weight of an item is its memory cost.

The objective is to select exactly one item (configuration) from each group (expert) to maximize the total value, without exceeding the knapsack’s capacity (memory budget).

3.2.3 MEASURING CONFIGURATION IMPACT VIA LAYER-WISE QUANTIZATION LOSS

A prerequisite for our ILP formulation is an efficient method to quantify the impact of thousands of potential (*bit, rank*) configurations, especially for MoE models with a large number of experts. As a full model evaluation for each candidate is computationally prohibitive, we propose an efficient proxy metric based on layer-wise quantization loss. Our approach is based on a simple idea: when we compress a single expert, the error this creates mostly affects that expert’s own layer. We measure this local error as the quantization error produced by compressing this expert.

Therefore, for each expert e_i and every candidate configuration c_j , we conduct an isolated perturbation experiment. In this step, only the target expert is temporarily replaced with its compressed counterpart corresponding to the candidate configuration, while the remainder of the model is held constant in FP16. The quantization loss for this configuration, denoted $QuantLoss(e_i, c_j)$, is then formally defined as the Euclidean (L2) distance between the output of this perturbed layer and its corresponding FP16 reference. This systematic process is repeated for all experts and configurations, yielding a comprehensive sensitivity map that serves as the primary input for our ILP solver.

The quantization loss for this configuration, $L_{i,j}$, is then formally defined as the Euclidean (L2) distance between the output of this perturbed layer and its corresponding FP16 reference:

$$L_{ij} = \|\text{LayerOutput}(e_i \leftarrow c_j) - \text{LayerOutput}_{\text{FP16}}\|_2.$$

This systematic process yields a comprehensive sensitivity map that serves as the primary input for our ILP solver, making the optimization computationally feasible.

3.2.4 INTEGER LINEAR PROGRAMMING FORMULATION

We formally define the optimization problem: Let $\mathcal{E} = \{e_1, e_2, \dots, e_N\}$ be the set of N experts in the model, and $\mathcal{C} = \{c_1, c_2, \dots, c_K\}$ be the set of K possible (*bit, rank*) configurations. To find the optimal (*bit, rank*) assignment, we formulate the problem as an optimization that seeks to minimize the total, importance-weighted quantization loss across all experts, subject to a strict memory budget. This allows us to systematically navigate the complex trade-offs between accuracy, expert sensitivity, and resource constraints.

Parameters.

- F_i : The activation frequency of expert e_i , serving as its importance weight.
- $L_{i,j}$: The layer-level quantization loss for expert e_i under compression configuration c_j .
- M_j : The memory overhead incurred by adopting configuration c_j .
- B : The total memory budget for the compression overhead.

324 **Decision Variable.** We introduce a binary variable $x_{ij} \in \{0, 1\}$, where $x_{ij} = 1$ if expert e_i is
 325 assigned configuration c_j , and 0 otherwise.
 326

327 **Objective Function.** Our goal is to minimize the sum of importance-weighted and quantization
 328 losses across all experts:
 329

$$\text{Minimize} \quad \sum_{i=1}^N \sum_{j=1}^K (F_i \cdot L_{ij}) \cdot x_{ij}. \quad (1)$$

332 **Constraints.** The optimization is subject to the following constraints:
 333

- 334 • Unique Choice Constraint: Each expert must be assigned exactly one configuration
 335

$$\sum_{j=1}^K x_{ij} = 1, \quad \forall i \in \{1, \dots, N\}. \quad (2)$$

- 339 • Memory Budget Constraint: The total memory overhead from all chosen configurations
 340 cannot exceed the budget
 341

$$\sum_{i=1}^N \sum_{j=1}^K M_j \cdot x_{ij} \leq B. \quad (3)$$

345 By adopting this two-stage approach, our framework fundamentally transforms the nature of the
 346 optimization problem. The initial brute-force search complexity of $O((|\mathcal{B}| \times |\mathcal{R}|)^{|\mathcal{E}|})$, is entirely
 347 circumvented. Instead, our method's complexity is dominated by two stages:

348 **(1) Quant Loss Collection:** The first stage involves populating the sensitivity map. This requires
 349 conducting an isolated perturbation experiment for each configuration across all experts. The com-
 350 plexity of this stage is polynomial: $O(|\mathcal{B}| \times |\mathcal{R}| \times |\mathcal{E}|)$, which is practically feasible.

351 **(2) ILP Solving:** The second stage involves solving the formulated ILP problem. Our formulation
 352 maps the challenge onto a well-structured Multiple-Choice Knapsack Problem (MCKP). For such
 353 problems, modern, highly optimized solvers can employ sophisticated techniques such as branch-
 354 and-bound and cutting-plane methods to find the provably optimal solution in a time frame that is
 355 vastly more efficient than the original brute-force search. In practice, for all our experiments, the
 356 solver finds the optimal configuration in under 10 seconds.

357 Finally, we solve this ILP problem using Google OR-Tools (SCIP) (Perron & Didier), formulating
 358 the objective to minimize the total weighted quantization loss. This process yields the globally
 359 optimal (bit, rank) assignment for the entire MoE model.

360 4 EXPERIMENT

363 4.1 EXPERIMENT SETUP

365 **Models.** We evaluate BT-MoE on three open-source MoE models: Mixtral-8x7B (Jiang et al., 2024),
 366 DeepSeek-V2-Lite (Liu et al., 2024), and Qwen1.5-MoE (Team, 2024). DeepSeek-V2-Lite employs
 367 a hybrid architecture, using dense MLP instead of MoE blocks in the first layer. More details about
 368 the models are provided in the Appendix A.1.

369 **Baselines.** We evaluate BT-MoE against three representative quantization methods, all configured
 370 with a group size of 128 for fair comparison: **HQQ** (Badri & Shaji, 2023), a calibration-free method
 371 using half-quadratic quantization; **GPTQ** (Frantar et al., 2022), a calibration-based approach lever-
 372 aging Hessian information for weight quantization; and **MiLo** (Huang et al., 2025a), a specialized
 373 MoE quantization method that utilizes low-rank compensators for extremely low-bit scenarios.

374 **Benchmarks.** We evaluate BT-MoE on five representative benchmarks, including Wikitext-2 (Mer-
 375 rity et al., 2017), HellaSwag (Zellers et al., 2019), PIQA (Bisk et al., 2020), Lambada (Radford et al.,
 376 2019), and MMLU (Hendrycks et al., 2021). We present the performance on MMLU with 5-shot
 377 and others with zero-shot. All evaluations are conducted using the EleutherAI Language Model
 378 Evaluation Harness (Gao et al., 2024).

378 4.2 COMPARISON OF MODEL PERFORMANCE AND MEMORY FOOTPRINT
379

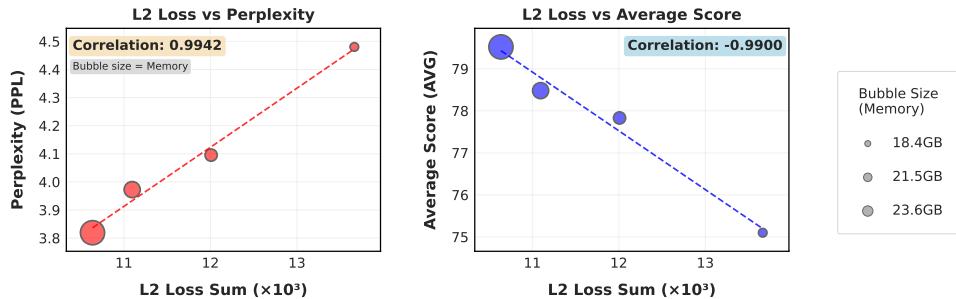
380 BT-MoE provides different compression configurations corresponding to various memory con-
381 straints. Each configuration individually sets the bit-width and compensator rank for every ex-
382 pert. Within these configurations, both the attention parts of the models and the shared experts in
383 DeepSeek-V2-Lite and Qwen1.5-MoE are uniformly set to a (4-bit, rank=512) configuration.

384 Table 1: Model Perplexity and Accuracy Perplexity under Various Quantization Methods.
385

Model	Method	Mem (GB)	WikiText2 (PPL)	HS	PQ	LO	MMLU	AVG
Mixtral-8x7B	FP16	88.90	3.700	86.02	83.67	80.87	71.34	80.48
	GPTQ-3bit	18.43	4.730	77.70	79.54	74.36	63.61	73.80
	HQQ-3bit	20.55	4.612	77.88	79.16	69.74	60.93	71.93
	MiLo	21.50	4.223	82.23	81.33	74.57	67.07	76.30
	BT-MoE	18.37	4.480	82.01	81.23	73.70	63.44	75.10
DeepSeek-MoE	FP16	31.24	5.832	77.33	79.00	73.88	45.07	68.82
	GPTQ-3bit	6.97	6.843	70.98	76.44	68.62	32.53	62.14
	HQQ-3bit	7.67	7.082	71.38	77.25	66.67	35.63	62.73
	MiLo	8.18	6.423	74.15	78.12	71.47	41.97	66.42
	BT-MoE	6.76	6.640	72.32	77.86	70.95	41.41	65.64
Qwen1.5-MoE	FP16	26.70	6.521	77.86	81.25	71.90	62.50	73.38
	GPTQ-3bit	6.73	8.293	72.77	76.80	62.33	54.36	66.56
	HQQ-3bit	6.83	8.272	72.46	77.15	62.48	51.29	65.85
	BT-MoE	6.83	7.377	74.54	78.31	67.75	56.71	69.35

404 To ensure fairness, we compare the accuracy of quantized models with different methods under
405 similar memory footprints. The comprehensive results, summarized in Table 1, show that BT-MoE
406 demonstrates superior performance compared to all baselines across all evaluated models.
407

408 On Mixtral-8x7B, BT-MoE shows significant advantages. At a memory footprint of 18.37 GB, our
409 method surpasses the slightly larger GPTQ-3bit baseline (18.43 GB) by over 1.3 points in average
410 accuracy. More impressively, our 20.36 GB configuration drastically outperforms HQQ-3bit (20.55
411 GB), reducing the WikiText2 perplexity from 4.612 to 4.095 and increasing the average score from
412 71.93 to 77.83, recovering a substantial portion of the performance gap to the FP16 model. This
413 result exemplifies our framework’s ability to establish a better accuracy-memory trade-off, with
414 consistent advantages observed across all tested models. More detailed and complete experimental
415 results are presented in the Appendix A.1.4.



426 Figure 6: The Objective Function Value as a proxy metric for final model performance on Mixtral-
427 8x7B. The bubble size represents the memory footprint of the compressed model under each quan-
428 tization configuration.

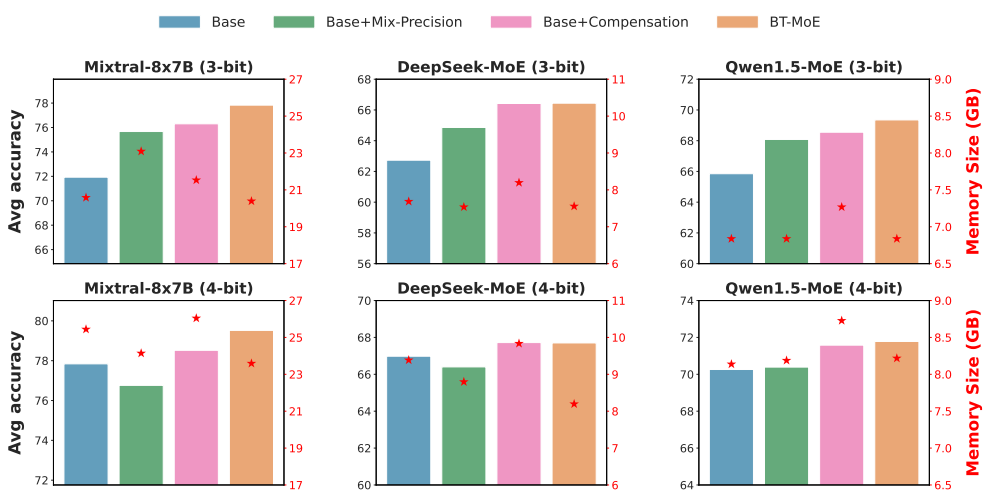
429 We validate that our ILP objective function, the Importance-Weighted L2 Loss Sum, serves as a
430 highly reliable proxy for final model performance. As shown in Figure 6, this predicted loss ex-
431 hibits a remarkable correlation of 0.9942 with Perplexity and -0.9900 with Average Score on various
432 datasets, confirming its effectiveness in guiding our optimization.

432 4.3 ABLATION STUDY
433

434 To quantify the individual contributions of mixed-precision and low-rank compensation within our
435 framework, we conduct an ablation study comparing our full BT-MoE method against two ablated
436 variants that represent each strategy in isolation. In Figure 7, the **Base** refers to the uniform-bit
437 quantization method. The **Base+Mix-Precision** represents a mixed-precision-only approach, which
438 allocates bit-widths based on an activation frequency heuristic without any compensators. The
439 **Base+Compensation** represents a compensation-only approach, applying low-rank compensators
440 to a uniform bit-width.

441 The results in Figure 7 reveal that the quality of heuristic-based mixed-precision is critically de-
442 pending on whether the heuristic itself can accurately measure expert importance. A clear example
443 of this limitation is on the Mixtral-8x7B model, where the frequency-based method fails to out-
444 perform the uniform-4bit HQQ baseline. As we discussed in Section 3.1, this is mainly because
445 Mixtral8x7B features a small number of experts with low variance in their activation frequencies,
446 making frequency an unreliable proxy for expert importance.

447 In contrast, our joint optimization method BT-MoE consistently achieves the best accuracy-memory
448 trade-off. On the DeepSeek-MoE model, for instance, while **Base+Compensation** achieves strong
449 accuracy, BT-MoE delivers comparable or better performance with a significantly smaller memory
450 footprint. This demonstrates that by jointly optimizing both bit-width and rank, BT-MoE can nav-
451 ige the complex trade-offs that simple heuristics cannot, validating the superiority of our global
452 optimization approach.



470
471 Figure 7: Results of different quantization methods and ours BT-MoE on various MoE models. The
472 * symbols denote the memory size of the compressed model.
473
474

475 5 CONCLUSION
476

477 In this study, we address the critical challenges of deploying MoE models with extreme compression.
478 We introduce BT-MoE, a novel framework that unifies the allocation of mixed-precision bit-widths
479 and low-rank compensators into a tractable Integer Linear Programming problem. We design an ob-
480 jective function to minimize the importance-weighted sum of quantization losses, which we validate
481 as a highly reliable predictor of final model performance. This budget-aware tuning approach sys-
482 tematically discovers a globally optimal configuration that maximizes model accuracy under a strict
483 memory budget. Our extensive experiments demonstrate that it consistently outperforms existing
484 quantization techniques by achieving higher accuracy at similar or even lower memory footprints.
485 These results highlight the potential of our unified optimization strategy to make the deployment of
486 large MoE LLMs more feasible in resource-constrained environments.

486 STATEMENT

487

488 ETHICS STATEMENT

489

490 This research was conducted using publicly available, open-source models and standard academic
 491 benchmarks, and did not involve the use of human subjects or private user data. Our work introduces
 492 BT-MoE, a compression technique for MoE models. Any ethical risks, such as potential biases or
 493 the generation of harmful content, are therefore inherited from the original models, as our work does
 494 not create new models.

495 REPRODUCIBILITY STATEMENT

496

497 To ensure the reproducibility of our work, we provide detailed information regarding the code,
 498 models, datasets, and experimental setup used in this paper. We also provide a README file with
 499 detailed reproduction instructions in our code submission.

500

501 REFERENCES

502

503 Hicham Badri and Appu Shaji. Half-quadratic quantization of large machine learning models,
 504 November 2023. URL https://mobiusml.github.io/hqq_blog/.

505

506 Yonatan Bisk, Rowan Zellers, Ronan Le Bras, Jianfeng Gao, and Yejin Choi. PIQA: reasoning
 507 about physical commonsense in natural language. In *The Thirty-Fourth AAAI Conference on
 508 Artificial Intelligence, AAAI 2020, The Thirty-Second Innovative Applications of Artificial Intel-
 509 ligence Conference, IAAI 2020, The Tenth AAAI Symposium on Educational Advances in Artifi-
 510 cial Intelligence, EAAI 2020, New York, NY, USA, February 7-12, 2020*, pp. 7432–7439. AAAI
 511 Press, 2020. doi: 10.1609/AAAI.V34I05.6239. URL <https://doi.org/10.1609/aaai.v34i05.6239>.

512

513 Zhen Dong, Zhewei Yao, Amir Gholami, Michael W. Mahoney, and Kurt Keutzer. HAWQ: hessian
 514 aware quantization of neural networks with mixed-precision. In *2019 IEEE/CVF International
 515 Conference on Computer Vision, ICCV 2019, Seoul, Korea (South), October 27 - November 2,
 516 2019*, pp. 293–302. IEEE, 2019. doi: 10.1109/ICCV.2019.00038. URL <https://doi.org/10.1109/ICCV.2019.00038>.

517

518 Haojie Duanmu, Xiuhong Li, Zhihang Yuan, Size Zheng, Jiangfei Duan, Xingcheng Zhang, and
 519 Dahua Lin. Mxmoe: Mixed-precision quantization for moe with accuracy and performance co-
 520 design. In *Forty-second International Conference on Machine Learning*, 2025. URL <https://openreview.net/forum?id=pXoZLGMNDm>.

521

522 Artyom Eliseev and Denis Mazur. Fast inference of mixture-of-experts language models with of-
 523 floating. *CoRR*, abs/2312.17238, 2023. doi: 10.48550/ARXIV.2312.17238. URL <https://doi.org/10.48550/arXiv.2312.17238>.

524

525 William Fedus, Barret Zoph, and Noam Shazeer. Switch transformers: Scaling to trillion parameter
 526 models with simple and efficient sparsity. *J. Mach. Learn. Res.*, 23:120:1–120:39, 2022. URL
 527 <https://jmlr.org/papers/v23/21-0998.html>.

528

529 Elias Frantar, Saleh Ashkboos, Torsten Hoefler, and Dan Alistarh. GPTQ: accurate post-training
 530 quantization for generative pre-trained transformers. *CoRR*, abs/2210.17323, 2022. doi: 10.
 531 48550/ARXIV.2210.17323. URL <https://doi.org/10.48550/arXiv.2210.17323>.

532

533 Leo Gao, Jonathan Tow, Baber Abbasi, Stella Biderman, Sid Black, Anthony DiPofi, Charles Fos-
 534 ter, Laurence Golding, Jeffrey Hsu, Alain Le Noac'h, Haonan Li, Kyle McDonell, Niklas Muen-
 535 nighoff, Chris Ociepa, Jason Phang, Laria Reynolds, Hailey Schoelkopf, Aviya Skowron, Lintang
 536 Sutawika, Eric Tang, Anish Thite, Ben Wang, Kevin Wang, and Andy Zou. The language model
 537 evaluation harness, 07 2024. URL <https://zenodo.org/records/12608602>.

538

539 Dan Hendrycks, Collin Burns, Steven Basart, Andy Zou, Mantas Mazeika, Dawn Song, and Jacob
 540 Steinhardt. Measuring massive multitask language understanding. In *9th International Confer-
 541 ence on Learning Representations, ICLR 2021, Virtual Event, Austria, May 3-7, 2021*. OpenRe-
 542 view.net, 2021. URL <https://openreview.net/forum?id=d7KBjmI3GmQ>.

540 Beichen Huang, Yueming Yuan, ZELEI SHAO, and Minjia Zhang. Milo: Efficient quantized moe
 541 inference with mixture of low-rank compensators. In *Eighth Conference on Machine Learning*
 542 and Systems, 2025a. URL <https://openreview.net/forum?id=NXVXiJmhe1>.

543

544 Wei Huang, Yue Liao, Jianhui Liu, Ruifei He, Haoru Tan, Shiming Zhang, Hongsheng Li, Si Liu,
 545 and Xiaojuan Qi. Mixture compressor for mixture-of-experts llms gains more. In *The Thirteenth*
 546 *International Conference on Learning Representations, ICLR 2025, Singapore, April 24-28, 2025*.
 547 OpenReview.net, 2025b. URL <https://openreview.net/forum?id=hheFYjOsWO>.

548 Albert Q. Jiang, Alexandre Sablayrolles, Antoine Roux, Arthur Mensch, Blanche Savary, Chris
 549 Bamford, Devendra Singh Chaplot, Diego de Las Casas, Emma Bou Hanna, Florian Bressand, Gi-
 550 anna Lengyel, Guillaume Bour, Guillaume Lample, Lélio Renard Lavaud, Lucile Saulnier, Marie-
 551 Anne Lachaux, Pierre Stock, Sandeep Subramanian, Sophia Yang, Szymon Antoniak, Teven Le
 552 Scao, Théophile Gervet, Thibaut Lavril, Thomas Wang, Timothée Lacroix, and William El Sayed.
 553 Mixtral of experts. *CoRR*, abs/2401.04088, 2024. doi: 10.48550/ARXIV.2401.04088. URL
 554 <https://doi.org/10.48550/arXiv.2401.04088>.

555 Muyang Li, Yujun Lin, Zhekai Zhang, Tianle Cai, Junxian Guo, Xiuyu Li, Enze Xie, Chenlin Meng,
 556 Jun-Yan Zhu, and Song Han. SVDQuant: Absorbing outliers by low-rank component for 4-
 557 bit diffusion models. In *The Thirteenth International Conference on Learning Representations*,
 558 2025a. URL <https://openreview.net/forum?id=vWR3KuiQur>.

559

560 Pingzhi Li, Xiaolong Jin, Zhen Tan, Yu Cheng, and Tianlong Chen. Quantmoe-bench: Examining
 561 post-training quantization for mixture-of-experts, 2025b. URL <https://arxiv.org/abs/2406.08155>.

562

563 Ji Lin, Jiaming Tang, Haotian Tang, Shang Yang, Wei-Ming Chen, Wei-Chen Wang, Guangxuan
 564 Xiao, Xingyu Dang, Chuang Gan, and Song Han. AWQ: activation-aware weight quantiza-
 565 tion for on-device LLM compression and acceleration. In Phillip B. Gibbons, Gennady Pekhi-
 566 menko, and Christopher De Sa (eds.), *Proceedings of the Seventh Annual Conference on Ma-*
 567 *chine Learning and Systems, MLSys 2024, Santa Clara, CA, USA, May 13-16, 2024*. mlsys.org,
 568 2024. URL https://proceedings.mlsys.org/paper_files/paper/2024/hash/42a452cba9dd64e9ba4aa95cc1ef21-Abstract-Conference.html.

569

570 Aixin Liu, Bei Feng, Bing Xue, Bingxuan Wang, Bochao Wu, Chengda Lu, Chenggang Zhao,
 571 Chengqi Deng, Chenyu Zhang, Chong Ruan, et al. Deepseek-v3 technical report. *CoRR*,
 572 abs/2412.19437, 2024. doi: 10.48550/ARXIV.2412.19437. URL <https://doi.org/10.48550/arXiv.2412.19437>.

573

574 Stephen Merity, Caiming Xiong, James Bradbury, and Richard Socher. Pointer sentinel mixture
 575 models. In *5th International Conference on Learning Representations, ICLR 2017, Toulon,*
 576 *France, April 24-26, 2017, Conference Track Proceedings*. OpenReview.net, 2017. URL <https://openreview.net/forum?id=Byj72udxe>.

577

578 Laurent Perron and Frédéric Didier. Cp-sat. URL https://developers.google.com/optimization/cp/cp_solver/.

579

580 Qwen, :, An Yang, Baosong Yang, Beichen Zhang, Binyuan Hui, Bo Zheng, Bowen Yu, Chengyuan
 581 Li, Dayiheng Liu, Fei Huang, Haoran Wei, Huan Lin, Jian Yang, Jianhong Tu, Jianwei Zhang,
 582 Jianxin Yang, Jiaxi Yang, Jingren Zhou, Junyang Lin, Kai Dang, Keming Lu, Keqin Bao, Kexin
 583 Yang, Le Yu, Mei Li, Mingfeng Xue, Pei Zhang, Qin Zhu, Rui Men, Runji Lin, Tianhao Li,
 584 Tianyi Tang, Tingyu Xia, Xingzhang Ren, Xuancheng Ren, Yang Fan, Yang Su, Yichang Zhang,
 585 Yu Wan, Yuqiong Liu, Zeyu Cui, Zhenru Zhang, and Zihan Qiu. Qwen2.5 technical report, 2025.
 586 URL <https://arxiv.org/abs/2412.15115>.

587

588 Alec Radford, Jeffrey Wu, Rewon Child, David Luan, Dario Amodei, Ilya Sutskever, et al. Language
 589 models are unsupervised multitask learners. *OpenAI blog*, 1(8):9, 2019.

590

591 Samyam Rajbhandari, Conglong Li, Zhewei Yao, Minjia Zhang, Reza Yazdani Aminabadi, Am-
 592 mar Ahmad Awan, Jeff Rasley, and Yuxiong He. Deepspeed-moe: Advancing mixture-of-experts
 593 inference and training to power next-generation AI scale. In Kamalika Chaudhuri, Stefanie

594 Jegelka, Le Song, Csaba Szepesvari, Gang Niu, and Sivan Sabato (eds.), *International Con-*
 595 *ference on Machine Learning, ICML 2022, 17-23 July 2022, Baltimore, Maryland, USA, vol-*
 596 *ume 162 of Proceedings of Machine Learning Research*, pp. 18332–18346. PMLR, 2022. URL
 597 <https://proceedings.mlr.press/v162/rajbhandari22a.html>.

598 Peng Tang, Jiacheng Liu, Xiaofeng Hou, Yifei Pu, Jing Wang, Pheng-Ann Heng, Chao Li, and
 599 Minyi Guo. HOBBIT: A mixed precision expert offloading system for fast moe inference. *CoRR*,
 600 [abs/2411.01433](https://arxiv.org/abs/2411.01433), 2024. doi: 10.48550/ARXIV.2411.01433. URL <https://doi.org/10.48550/arXiv.2411.01433>.

601 602 Qwen Team. Qwen1.5-moe: Matching 7b model performance with 1/3 activated parameters, Febru-
 603 ary 2024. URL <https://qwenlm.github.io/blog/qwen-moe/>.

604 605 Kuan Wang, Zhijian Liu, Yujun Lin, Ji Lin, and Song Han. HAQ: hardware-aware automated quan-
 606 tization with mixed precision. In *IEEE Conference on Computer Vision and Pattern Recognition,*
 607 *CVPR 2019, Long Beach, CA, USA, June 16-20, 2019*, pp. 8612–8620. Computer Vision Founda-
 608 tion / IEEE, 2019. doi: 10.1109/CVPR.2019.00881. URL http://openaccess.thecvf.com/content_CVPR_2019/html/Wang_HAQ_Hardware-Aware_Automated_Quantization_With_Mixed_Precision_CVPR_2019_paper.html.

609 610 611 612 613 614 615 616 617 618 619 620 621 622 623 624 625 626 627 628 629 630 631 632 633 634 635 636 637 638 639 640 641 642 643 644 645 646 647 Guangxuan Xiao, Ji Lin, Mickael Seznec, Hao Wu, Julien Demouth, and Song Han. Smoothquant:
 Accurate and efficient post-training quantization for large language models. In Andreas Krause,
 Emma Brunskill, Kyunghyun Cho, Barbara Engelhardt, Sivan Sabato, and Jonathan Scarlett
 (eds.), *International Conference on Machine Learning, ICML 2023, 23-29 July 2023, Honolulu,*
Hawaii, USA, volume 202 of *Proceedings of Machine Learning Research*, pp. 38087–38099.
 PMLR, 2023. URL <https://proceedings.mlr.press/v202/xiao23c.html>.

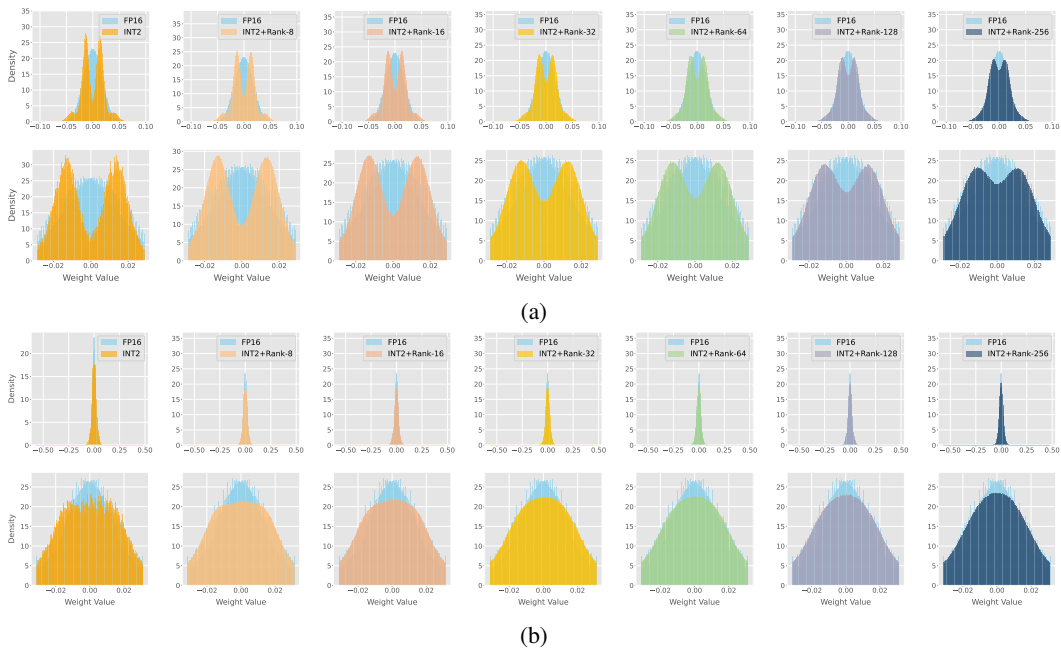
Zhewei Yao, Xiaoxia Wu, Cheng Li, Stephen Youn, and Yuxiong He. Exploring post-training quan-
 tization in llms from comprehensive study to low rank compensation. In Michael J. Wooldridge,
 Jennifer G. Dy, and Sriraam Natarajan (eds.), *Thirty-Eighth AAAI Conference on Artificial Intel-*
ligence, AAAI 2024, Thirty-Sixth Conference on Innovative Applications of Artificial Intelligence,
IAAI 2024, Fourteenth Symposium on Educational Advances in Artificial Intelligence, EAAI 2014,
February 20-27, 2024, Vancouver, Canada, pp. 19377–19385. AAAI Press, 2024. doi: 10.1609/aaai.V38I17.29908. URL <https://doi.org/10.1609/aaai.v38i17.29908>.

Zhihang Yuan, Yuzhang Shang, Yue Song, Qiang Wu, Yan Yan, and Guangyu Sun. ASVD:
 activation-aware singular value decomposition for compressing large language models. *CoRR*,
[abs/2312.05821](https://arxiv.org/abs/2312.05821), 2023. doi: 10.48550/ARXIV.2312.05821. URL <https://doi.org/10.48550/arXiv.2312.05821>.

Rowan Zellers, Ari Holtzman, Yonatan Bisk, Ali Farhadi, and Yejin Choi. Hellaswag: Can a ma-
 chine really finish your sentence? In Anna Korhonen, David R. Traum, and Lluis Marquez
 (eds.), *Proceedings of the 57th Conference of the Association for Computational Linguistics, ACL 2019, Florence, Italy, July 28- August 2, 2019, Volume 1: Long Papers*, pp. 4791–
 4800. Association for Computational Linguistics, 2019. doi: 10.18653/V1/P19-1472. URL
<https://doi.org/10.18653/v1/p19-1472>.

648 **A APPENDIX**649 **A.1 FULL EXPERIMENTAL RESULTS**650 **A.1.1 MODEL DETAILS IN EXPERIMENT**651 **Table 2: Architectural Specifications of Evaluated MoE Models**

652 Model	653 Params (GB)	654 Experts	655 TopK
Mixtral-8x7B	92.9	8	2
Qwen1.5-MoE	26.7	60 + 4	4
DeepSeek-V2-Lite	29.3	64 + 2	6

661 **A.1.2 THE EFFECT OF COMPENSATOR RANK ON THE ACCURACY RECOVERY OF LOW-BIT
662 QUANTIZED WEIGHTS**674 **Figure 8: The progressive recovery of weight distributions for different model components under
675 aggressive INT2 quantization. The top set of plots (a) shows the distributions for an expert's weights,
676 while the bottom set (b) shows distributions for attention weights. Each column corresponds to a
677 different compensator rank, from Rank-0 to Rank-256.**688 **A.1.3 OFFLINE COMPUTATIONAL COST FOR DATA COLLECTION**694 Our framework requires a one-time, offline data collection phase to generate the sensitivity map (the
695 $L_{i,j}$ values) used by the ILP solver. This involves performing an isolated perturbation experiment
696 for every expert across all candidate (bit, rank) configurations, as described in Section 3.2.3.697 On a single NVIDIA A100 GPU, this data collection process takes approximately 4 to 12 hours,
698 with the duration depending on the total number of experts in the MoE model (e.g., Mixtral-8x7B is
699 on the lower end, while DeepSeek-MoE is on the higher end). It is important to note that while this
700 upfront data collection is computationally intensive, it is a one-time cost. Once this comprehensive
701 sensitivity map is generated, the ILP optimization itself is extremely efficient, consistently finding
the globally optimal configuration in under 10 seconds.

702 A.1.4 FULL EXPERIMENTAL RESULTS UNDER DIFFERENT MEMORY CONSTRAINTS
703704 Table 3: The full results of GPTQ, HQQ, MiLo, MPQ-Freq and ours BT-MoE with 3-bit and 4-bit
705 weight quantization among 5 datasets on Mixtral-8x7B, DeepSeek-MoE-16B and Qwen1.5-MoE-
706 14B. We evaluate on the following datasets: Wikitxt-2, HellaSwag(HS), LAMBADA-openai(LO),
707 PIQA(PQ) and MMLU. Specifically, the GPTQ method utilizes Wikitext2 as the calibration dataset.
708 MPQ-Freq is a heuristic mixed-precision-only strategy, which allocates bit-widths based on activation
709 frequency without any compensators.

710 Model	711 Bits	712 Memory	713 WikiText2(PPL)	714 HS	715 PQ	716 LO	717 MMLU	718 AVG
719 Mixtral-8x7B	FP16	88.90G	3.700	86.02	83.67	80.87	71.34	80.48
	GPTQ-4bit	23.81G	4.233	80.73	81.44	74.42	67.84	76.11
	GPTQ-3bit	18.43G	4.731	77.70	79.54	74.36	63.61	73.80
	HQQ-4bit	25.41G	3.941	83.65	82.62	76.57	68.53	77.84
	HQQ-3bit	20.55G	4.612	77.88	79.16	69.74	60.93	71.93
	MiLo	21.50G	4.223	82.23	81.33	74.57	67.07	76.30
	MiLo	26.01G	3.774	85.47	83.18	77.31	68.13	78.52
	MPQ-Freq	23.06G	4.777	82.02	82.37	72.23	66.07	75.67
	MPQ-Freq	24.11G	4.354	82.77	82.53	74.70	67.07	76.76
	BT-MoE	18.37G	4.4803	82.01	81.23	73.70	63.44	75.10
720 DeepSeek-MoE	BT-MoE	20.36G	4.0953	84.64	83.03	76.88	66.76	77.83
	BT-MoE	21.50G	3.9725	85.04	83.08	77.99	67.79	78.48
	BT-MoE	23.56G	3.8191	85.57	83.51	79.39	69.60	79.52
	FP16	31.24G	5.832	77.33	79.00	73.88	45.07	68.82
	GPTQ-4bit	8.75G	6.266	74.67	78.14	72.28	42.23	66.83
	GPTQ-3bit	6.97G	6.843	70.98	76.44	68.62	32.53	62.14
	HQQ-4bit	9.37G	6.187	74.68	78.61	72.32	42.30	66.98
	HQQ-3bit	7.67G	7.082	71.38	77.25	66.67	35.63	62.73
	MiLo	8.18G	6.423	74.15	78.12	71.47	41.97	66.42
	MiLo	9.82G	5.946	76.74	78.83	72.11	43.21	67.72
721 Qwen1.5-MoE	MPQ-Freq	7.52G	6.543	72.45	78.00	68.95	40.05	64.86
	MPQ-Freq	8.78G	6.319	74.39	78.07	70.95	42.19	66.40
	BT-MoE	6.76G	6.640	72.32	77.86	70.95	41.41	65.64
	BT-MoE	7.54G	6.348	73.71	78.13	71.94	41.98	66.44
	BT-MoE	8.18G	6.180	75.51	78.83	73.51	42.93	67.70
	FP16	26.70G	6.521	77.86	81.25	71.90	62.50	73.38
	GPTQ-4bit	8.03G	7.544	75.61	78.40	64.46	58.25	69.18
	GPTQ-3bit	6.73G	8.293	72.77	76.80	62.33	54.36	66.56
	HQQ-4bit	8.13G	7.143	75.60	78.65	67.22	59.58	70.26
	HQQ-3bit	6.83G	8.272	72.46	77.15	62.48	51.29	65.85
722 Qwen1.5-MoE	MiLo	7.26G	7.326	75.24	78.40	66.28	55.28	68.55
	MiLo	8.72G	6.860	77.32	79.64	70.99	58.45	71.58
	MPQ-Freq	6.83G	7.667	73.81	78.00	65.44	55.08	68.08
	MPQ-Freq	8.18G	7.062	75.32	78.40	69.60	58.22	70.39
	BT-MoE	6.83G	7.377	74.54	78.31	67.75	56.71	69.35
723	BT-MoE	8.21G	6.880	76.37	79.43	71.16	60.17	71.78

745 A.2 THE USE OF LARGE LANGUAGE MODELS (LLMs)

746 During the preparation of this manuscript, the authors utilized Large Language Models (LLMs)
747 as a writing assistant. The primary use of these tools was for language enhancement, including
748 improving grammar, clarity, and readability through translation and polishing of the text.749
750
751
752
753
754
755